Solar Energy Materials & Solar Cells 282 (2025) 113412

Contents lists available at ScienceDirect

Solar Energy Materials and Solar Cells

journal homepage: www.elsevier.com/locate/solmat

Silver reduction through direct wire bonding for Silicon Heterojunction solar cells

Yanxin Liu [a,b,*], Ian Marius Peters [a], Kaining Ding [a,b], Bart Pieters [a], Karsten Bittkau [a], Uwe Rau [a,b], Mohamed Issifi Yacouba [a], Henrike Gattermann [a], Volker Lauterbach [a], Andreas Lambertz [a,**]

[a] IMD-3: Photovoltaics, Forschungszentrum Jülich GmbH, Wilhelm-Johnen Straße, 52425, Jülich, Germany
[b] Jülich Aachen Research Alliance (JARA-Energy) and Faculty of Electrical Engineering and Information Technology, RWTH Aachen University, Schinkelstr. 2, 52062, Aachen, Germany

ARTICLE INFO

Keywords:
Direct wire bonding
Silicon heterojunction (SHJ) solar cells
Copper wires
Conductive paste
Cost reduction

ABSTRACT

This study introduces Direct Wire Bonding (DWB) as a low-temperature method for interconnecting finger-free Silicon Heterojunction (SHJ) solar cells using low-cost, highly conductive copper wires. The wires are attached to the SHJ cells via discrete pads of conductive paste, enabling direct current extraction from the indium tin oxide (ITO) layer and facilitating transport to sequentially connected cells. We describe the DWB fabrication process and demonstrate its potential by comparing its performance to that of traditional SHJ modules. Our test devices show that DWB modules achieve competitive efficiencies, 0.03 % abs. higher in experiments than the 0BB and multi-wire solutions—while significantly reducing material consumption. In the study we give an outlook on the possible improvement in efficiency. The economic analysis further demonstrates that DWB can reduce production costs to as low as 18 % of the cost of other SHJ metallization and interconnection techniques. These initial results suggest that DWB is a cost-effective solution that addresses both economic and material scarcity challenges in the photovoltaic industry.

1. Introduction

Amid the pressure of the climate crisis, nations worldwide have agreed to the Paris Accords [1] to mitigate greenhouse gas emissions. As a promising renewable energy source, photovoltaic power is considered a viable alternative to traditional energy sources and is widely utilized in power plants. By 2023, global photovoltaic shipments reached approximately 400 GW, with PERC technology maintaining its dominance in the industry, as depicted in Fig. 1. Under the greenhouse gas emissions requirements of the Accords, the ITRPV predicts that annual photovoltaic production will reach terawatt level by 2030, resulting in the phase out of less efficient passivated emitter and rear cell (PERC) technology in favor of the emerging tunnel oxide passivated contact (TOPCon) and SHJ technologies [2]. However, this rapid growth and new cell technologies could lead to shortages of raw materials for photovoltaics, potentially causing price fluctuations. Based on the current silver (Ag) usage for the new cell concepts, particularly for SHJ solar cells, it is predicted that the industry will consume about half of the annual silver supply once production reaches the terawatt era [3]. Besides silver, bismuth (Bi) as the key element in the low temperature solder particular for interconnection of SHJ solar cells is also a concern. Even if only SHJ solar cells adopt bismuth-based soldering in 2034, the photovoltaic industry could consume about 25 % of the global annual bismuth supply in 2034, assuming a rate of 13 mg/W [3,4]. Therefore, reducing consumption of silver paste and rare elements for interconnection is crucial for the photovoltaic industry, particularly for SHJ solar cells.

In the traditional SHJ photovoltaic production process, solar cells are initially metallized to laterally enhance current transport. Once electrical carriers accumulate at the busbars from fingers on the cell, they are collected via soldered copper wires or ribbons for the electrical transport to the next cell. This study explores the possibility of direct extraction of current from the ITO layer of SHJ solar cells using conductive paste applied in discrete pads, subsequently transported via thin, highly conductive copper wires. Additionally, the wires extending

* Corresponding author. IMD-3: Photovoltaics, Forschungszentrum Jülich GmbH, Wilhelm-Johnen Straße, 52425, Jülich, Germany.
** Corresponding author.
E-mail addresses: ya.liu@fz-juelich.de (Y. Liu), a.lambertz@fz-juelich.de (A. Lambertz).

https://doi.org/10.1016/j.solmat.2025.113412
Received 29 October 2024; Received in revised form 2 January 2025; Accepted 6 January 2025
Available online 12 January 2025

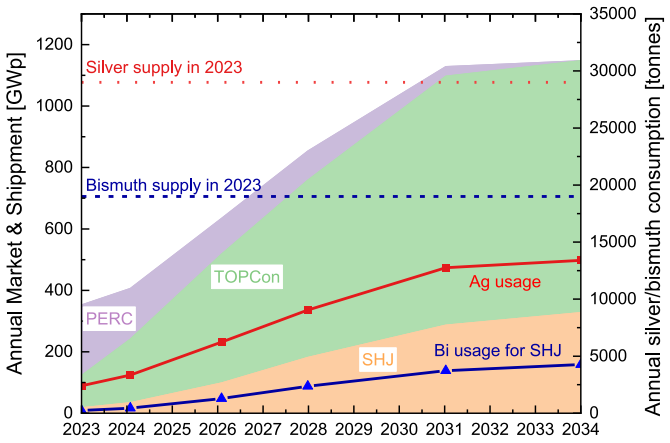

Fig. 1. The forecast of different cell technologies in the PV market and shipment is shown in a stacked area chart, with corresponding Ag consumption for PV (red line) and Bi consumption if all SHJ use Bi-based low-temperature solder (blue line) [2,3,5]. (For interpretation of the references to colour in this figure legend, the reader is referred to the Web version of this article.)

from the cell can still be used for interconnection with the next cell as depicted in Fig. 2. Therefore, this method has the potential to eliminate the need for low-temperature solder and minimize the use of silver. Maximizing the device's power output is critical, necessitating careful design of the front electrode with wires and pads. We, therefore, model the module with Direct Wire Bonding (DWB) using PVMOS [6] and calculate the optimal pitch of pads and wires. To compare with another metallization scheme and analyze power dissipation, modules with wires interconnection at 0.828 cm pitch and ribbon interconnections at 1.65 cm pitch are simulated as references. Finally, the DWB module, optimized with specific parameters, demonstrates performance comparable to the reference method in the experiment. Since there is no requirement for optical shading in the metallization and interconnection on the rear side of solar cells, making implementation easier, this paper will exclusively focus on direct wire bonding (DWB) on the front side of solar cells and compare it to traditional metallization and interconnection methods.

2. The fabrication of the device

All solar cells used in the experiment are from the same batch of M2+ commercial metallization-free SHJ solar cells. Initially, the cells are screen-printed with a 0-busbar metallization layout featuring 250 fingers on the rear side. The cells are cut into 5 × 5 cm squares from the edge, leaving only three non-passivated edges leading to some efficiency losses. After attaching copper wires with a diameter of 30 μm to both ends of the cell, silver coated copper paste is dispensed in tiny dots along the wires at a specified pitch by a dispensing robot. During dispensing, the cone-shaped nozzle with a 150 μm opening is aligned with the wires, 50 μm above the cell. Electrical loss and optical shading in the device are inversely affected by the wire diameter, wire pitch, and dot pitch, necessitating careful optimization of these variables by simulation, which will be detailed in the next section. After connecting six 250 μm diameter copper (Cu) tabbing wires coated with low-temperature solder wires with a pitch of 8.28 mm for the back contact, the cell is laminated in a module in a size of 20 × 20cm at 150 °C for 1060 s, during which the paste is annealed, as shown in Fig. 3(a).

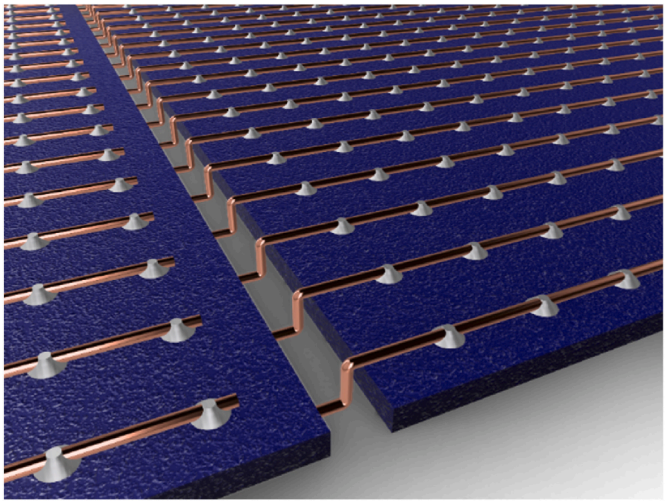

Fig. 2. The concept of direct wire bonding (DWB) on SHJ solar cells.

For comparison, the metallization-free M2+ SHJ solar cells are screen-printed with 96 fingers on the front side and 250 fingers in the same arrangement as DWB samples on the back. After cutting, six tabbing wires the features described previously are bonded to both sides of the 5 × 5 cm cells, corresponding to 18 tabbing wires on an M2+ solar cell as depicted in Fig. 3(b). To mimic the common 9 busbars interconnection layout on M2+ solar cells, three 1 mm wide Ag-coated Cu ribbons are attached to the printed busbars of the cut cells using electrically conductive adhesive dispensed in dots with a pitch of 1.65 cm shown in Fig. 3(c).

3. Device simulation and optimization

Table 1 shows the contact and line resistances of metallization and interconnection as measured in the experiment. The line resistance of the Cu wire is about six times lower than that of an Ag finger, and 13 times lower than that of fingers from Ag-coated Cu paste, meeting the requirements for longer-distance current transport on cells and potentially substituting tabbing for the scale of cells in the experiment. In addition to line resistance for lateral current transport, vertical electrical loss at the contact points between wires and ITO is also critical. The Ag-coated Cu paste exhibits a slightly lower (3.35 mΩ cm^2) contact resistance than the Ag paste used in the experiment. This is probably due to the 2.4%wt higher solid content or the particle size distribution in the Ag-coated Cu paste. Combining the benefits of Ag-coated Cu paste at the contact points with the lower line resistance of Cu wires, DWB is promising in achieving performance comparable to traditional metallization and interconnection methods. The slight difference in contact resistance may be attributed to the different measurement structures used. Contact resistance of wires to ITO in DWB samples is measured using the Cross Bridge Kervin Resistor (CBKR) method, whereas the contact resistance of paste is characterized using the transmission line measurement (TLM) structure [7].

Since all devices are benchmarked against the performance of reference modules with six tabbing wires on each side in the experiment, simulating and optimizing the DWB structure requires accounting for the optical and cell conditions of the reference. Typically, our solar module without anti-reflection coating on the front glass can achieve 20.9 % module efficiency using the M2+ SHJ solar cell with 23.5 % efficiency, when measured with an aperture to prevent light collection from the surrounding white backsheet, resulting in a short circuit current (J_{sc}) of 36.06 mA/cm^2. For this study, we cut the solar cells into 5 × 5 cm^2 pieces, resulting in a decrease in fill factor (*FF*)and open-circuit voltage (V_{oc}), leading to a reduction in average efficiency from 23.3 % to 22.5 %. The modules are measured using a 5 × 5 cm^2 aperture due to the aforementioned reasons, leading to a J_{sc} of 35.66 mA/cm^2 for the reference six-wire solar modules. The pads of the DWB device are printed using dispensing technology. The final dot dimensions are highly sensitive to the nozzle-to-surface gap, wire alignment (influenced by wire straightness and table levelness), and dispenser robot precision. This sensitivity leads to printed pads with varying shapes (ranging from circular to square) and sizes (200–300 μm), as shown magnified in Fig. 3

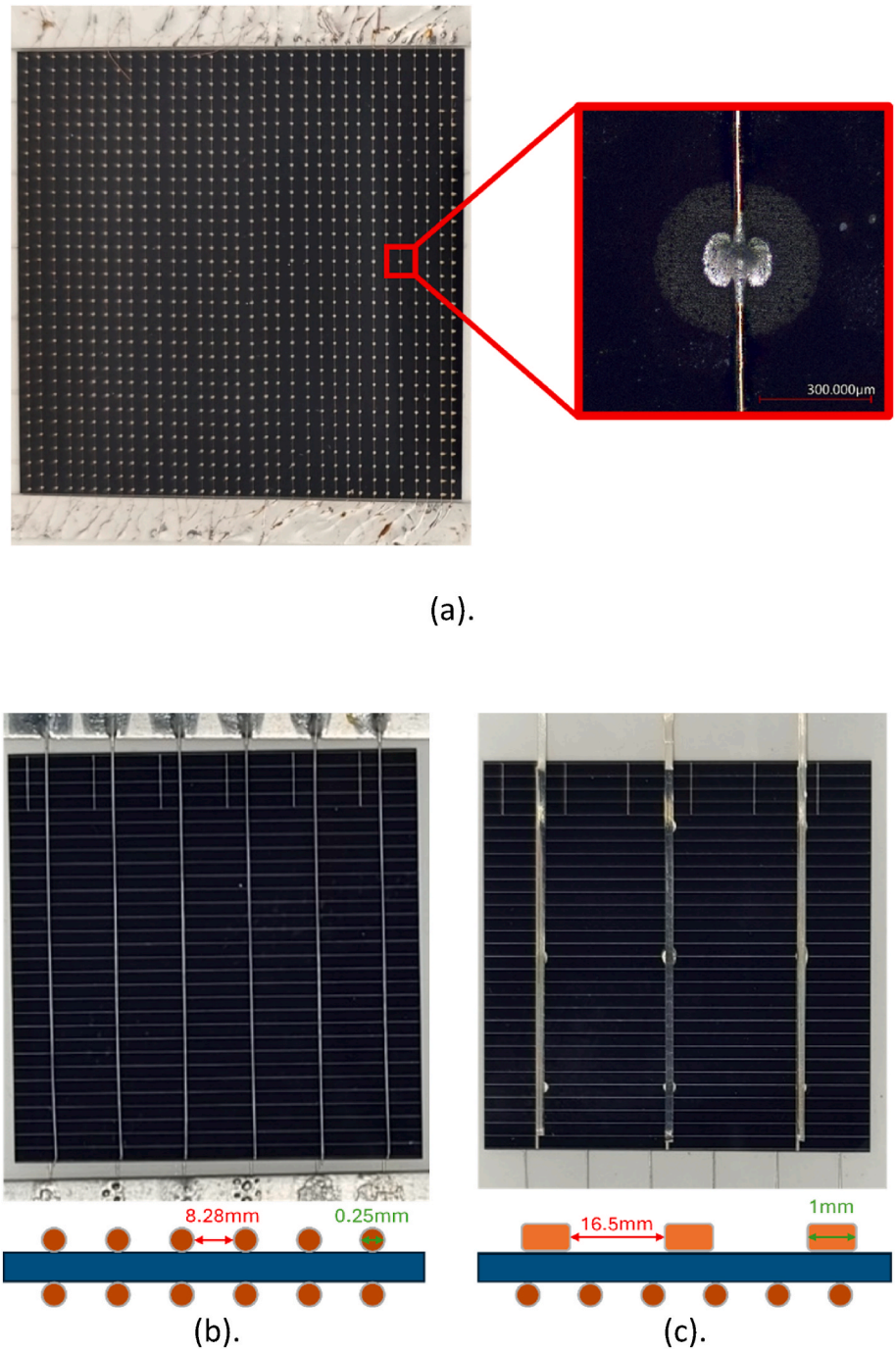

Fig. 3. Photos and schematic cross-section of the test devices, a) DWB solar module with a magnified view of a connection pad, b) Solar module with 6 tabbing wires on both sides, equivalent M2+ solar module with 18 tabbing wires and c) Solar module with 3 tabbing ribbons on the front side, equivalent M2+ solar module with 9 tabbing ribbons.

Table 1
Contact resistivity and line resistivity of DWB method and two different fingers screen printed with screen opening 35 µm.

	Contact resistivity [mΩ·cm^2]	Line resistivity [Ω/cm]
Fingers made of Ag paste	13.49	1.61
	10.14	3.21
Fingers made of Ag-coated Cu paste		
	10.20	0.24
DWB (Cu wires through Ag coated Cu paste to ITO)		

(a). Because these variations are difficult to predict precisely, we modelled the dots as 300 µm squares in our simulations to maintain simplicity and consistency.

Simulated efficiency of the DWB module as a function of wire pitch and number of contact pads is illustrated in Fig. 4. The DWB method achieves a maximum efficiency of 20.19 % with a wire pitch of 1.4 mm and 34 contact pads per wire, compared to the reference module, which achieves 20.43 % efficiency in simulation with six tabbing wires on front side. Increasing the number of wires or contact pads enhances the fill factor, though it results in performance loss due to optical shading. Similarly, Fig. 5 plots the maximum efficiency that optimized DWB modules can achieve with varying wire diameters. When wire diameters

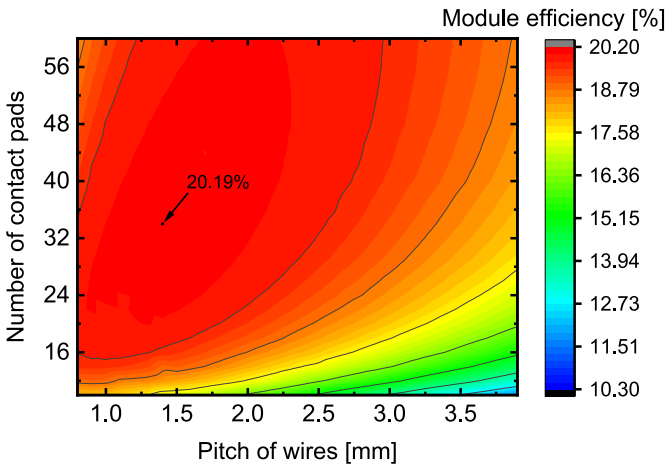

Fig. 4. Simulated efficiency of the DWB module varies across different wire pitches and numbers of contact pads. Under the optical conditions of the reference modules, the maximum module efficiency can reach 20.19 %.

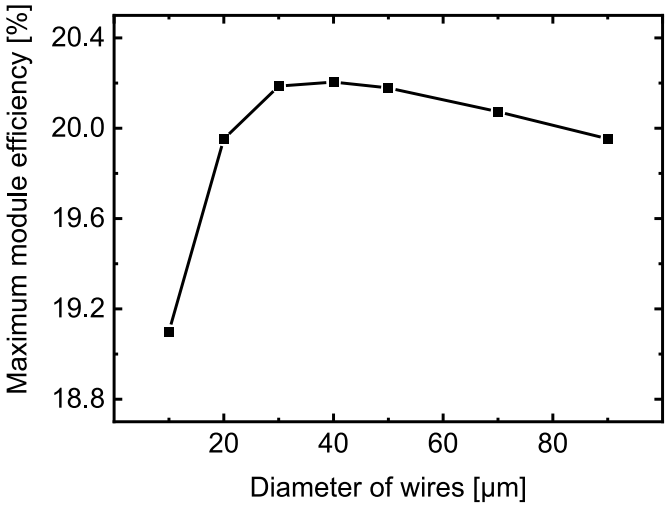

Fig. 5. Maximum efficiency of optimized DWB modules versus varying wire diameters.

range from 30 μm to 50 μm, the highest efficiency fluctuates by 0.1%rel., peaking at 40 μm with an efficiency of 20.20 %. However, when wire diameters are less than 40 μm, device efficiency is significantly limited by wire conductivity, whereas the efficiency decrease from shading with diameters exceeding 40 μm is less pronounced.

4. Experiment result and analysis

Using the optimized parameters for DWB modules, the actual and simulated performance of modules with various metallization and interconnection methods was compared, as shown in Fig. 6. All solar modules in the experiment demonstrated efficiencies of approximately 20.5 % in Fig. 6(a) (the rather low efficiency is related to the light guiding effect of the glass when using relatively small solar cells). The DWB modules exhibited an average efficiency approximately 0.03 % abs higher than modules with six tabbing wires and 0.1 % abs higher than those with three tabbing ribbons on the front side. However, simulation results suggest that DWB modules should perform between the modules with six tabbing wires and 3 tabbing ribbons interconnection scheme.

The discrepancy between simulation and experimental results is also evident in the short-circuit current density (*Jsc*) in Fig. 6(b), which follows the same trend. While the simulated *Jsc* for all devices is approximately 35 mA/cm^2, the DWB modules achieved the highest experimental *Jsc* of 36.02 mA/cm^2, which is 0.37 mA/cm^2 and 1.02 mA/cm^2 higher than the modules with six tabbing wires and three tabbing ribbons, respectively. The underestimation of short-circuit current in the simulation can be attributed to two factors. First, the simulation did not account for light reflection caused by the reddish wires[8] and cone-shaped dots, as shown in Fig. 3(a). Secondly, as mentioned in the simulation section, some pads may be smaller than those in the model, likely leading to an overestimation of the shading effect of the dots. In addition, a difference of 0.7 mA/cm^2 in *Jsc* was observed in modules with three tabbing ribbons between experiment and simulation. It can be attributed to the surface structure which scatters the light of the 1 mm interconnection ribbons.

In contrast, open-circuit voltage (*Voc*) and fill factor (*FF*), depicted in Fig. 6(c) and **(d)**, show close agreement between simulation and experiment. The *Voc* remained consistent from cell to module, with all modules measuring approximately 735 mV. As calculated by PVMOS, the primary limitation of the DWB device is its fill factor (*FF*), which is approximately 2.5 % absolute lower in simulation and 0.7 % absolute lower in experiments compared to the other two other schemes. This is attributed to the longer current transfer distance within the ITO layer to reach the contact dots, compared to other designs. Given further trade-off between current and ohmic loss is still possible in the DWB device, the use of a more conductive, but less transparent, ITO layer may be an effective strategy for performance enhancement.

5. Silver usage and cost analysis

The weight of the paste used in the experiment is determined by measuring the volume of the metallization with a confocal microscope and multiplying by the density, then expressed in mg/W, based on the assumption of modules with 20 % efficiency. The usage of paste on the front side of modules in this study is illustrated in Fig. 7 alongside the levels of different cell technologies in the industry. The paste applied in the 0BB layouts is close to that observed in industrial SHJ solar cells and marginally higher than PERC cells on the front side, which have the lowest Ag consumption. The busbars in the 3BB samples are dispensed with a greater thickness than is typical of industrial busbars. Consequently, the paste consumption in the 3BB samples is 3.7 mg/W higher than in 0BB solar cells.

The weight per dot in the DWB sample is measured in the way about 0.002 mg, which corresponds to 4.25 mg/W, lower than in the 0BB layout, at 3.09 mg/W. Moreover, the Ag-coated Cu paste used in the DWB solar module contains 40 % copper, leading the silver usage in the DWB module is only 2.55 mg/W about one third of that in the 0BB module design. As this is the first demonstration of the concept, the amount of paste used in the DWB can be significantly reduced by employing smaller dots. Moving forward, if the dots are printed with a diameter of 150 μm and a thickness of 15 μm—achievable through screen printing or jet dispensing—the paste consumption could be reduced to 2.8 mg/Wp, and the mass of silver on the front side of the modules could drop to 1.7 mg/W. Assuming the paste usage on the front is about 58 % of the paste on the back as traditional SHJ metallization layout, total Ag usage could be reduced to 4.63 mg/W, meeting the intermediate goal 5 mg/W for silver usage [3,9].

The material cost analysis of metallization and interconnection on the front side is shown in Fig. 8. PERC and TOPcon, as high-temperature solar cells, enable the use of traditional soldering processes. In contrast, the SHJ industry employs conductive gluing or low-temperature soldering processes, such as Smartwire interconnection. Since the Smartwire used in the 0BB solar module is not commercially available due to patent issues, the cost data for interconnection in this experiment are from literature [9]. The wires in the DWB design can also be used for series interconnection of the solar cells; thus, the DWB costs include only the paste and Cu wires. The DWB benefits from using Ag-coated Cu paste, which costs about 350 euros/kg—approximately 44 % of the price

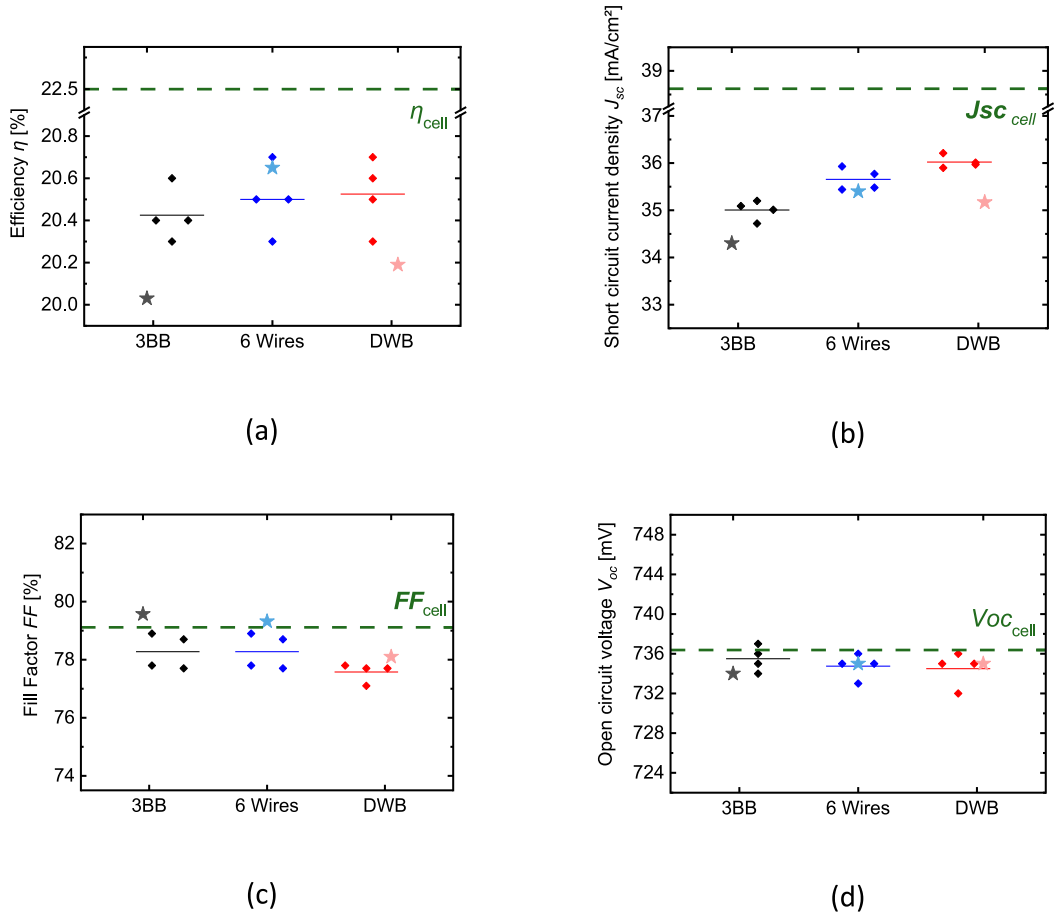

Fig. 6. a) The Efficiency b) Fill factor c) Short circuit current density and d) Open circuit voltage of modules using different metallization and interconnection methods measured with aperture. The green dashed lines represent the average performance of the solar cells after cutting. The stars are the simulated results. (For interpretation of the references to colour in this figure legend, the reader is referred to the Web version of this article.)

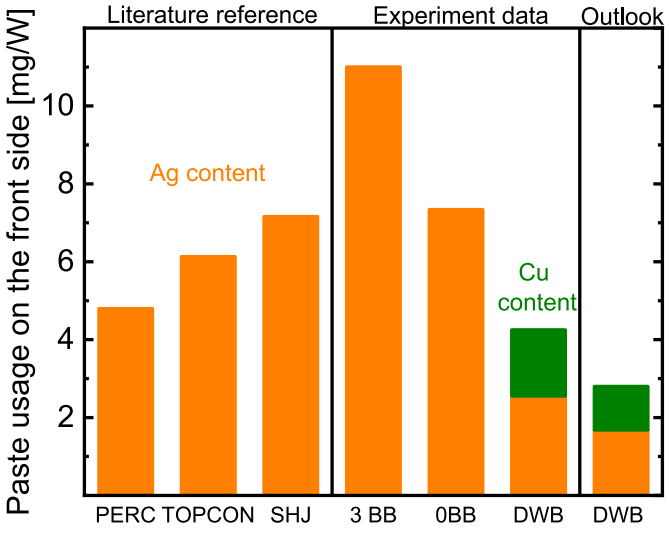

Fig. 7. The consumption of paste in the experiment and industry [5].

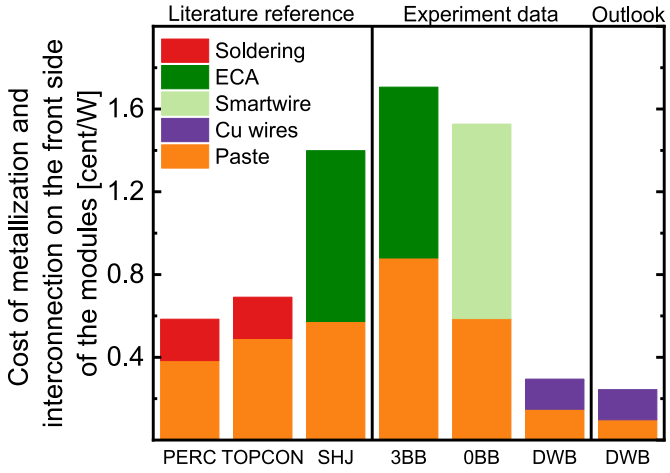

Fig. 8. Costs of materials and processes for metallization and interconnection on the front side [5,9].

of conventional Ag paste. Moreover, the 30 μm wires used in the DWB cost about 70 euros/kg, ten times less than Ag paste. Generally, the cost of SHJ solar modules is higher than that of TOPcon and PERC, due to higher Ag paste usage and more expensive interconnection methods. However, the DWB method avoids the cost of additional interconnections, which require costly bismuth or indium in low-temperature solder, or even larger amounts of silver (Ag) in electrically conductive adhesives (ECAs). Consequently, it achieves a cost that is up to 18 % of the cost of other SHJ interconnection solutions, at 0.30 euro cents/Wp. With projected improvements, the cost could decrease to 0.24 euro cents/Wp, making it even more cost-effective than

the metallization and interconnection of the PERC technology.

6. Summary and outlook

This study demonstrated the connection of low-cost Cu wires on SHJ solar cells as electrodes with conductive paste applied in discrete pads to replace the traditional metallization and interconnection process. The paste used in this structure is cured at low temperatures during the lamination process, making it suitable for SHJ and perovskite-Si tandem solar cells. As a proof of concept, we have achieved module efficiency higher than those of the 6-wire and 3-ribbon interconnection schemes on a 5 × 5 cm SHJ solar cell by optimizing the design through simulation. In terms of paste consumption, it is comparable to modules with the lowest usage 0BB solution. However, the DWB offers superior cost savings by eliminating the need for interconnect material. Looking ahead, the optimum could shift in favor of DWB by using a TCO with higher conductivity or by minimizing the diameter of pads and correspondingly increasing their number and wires. Additionally, the cost of DWB could be further reduced by adopting printing techniques that thin the pads of paste. Moreover, since the paste in DWB primarily serves as the interface between the wires and ITO, using a less conductive paste, like carbon paste, that still maintains low contact resistance could be feasible, potentially further reducing costs. As this is an initial exploration of DWB, industrial-scale implementation remains to be fully explored. However, as the device is scaled up, the optimal wire thickness is expected to increase to accommodate higher current flow. For stringing, we propose the following strategy: After wires are applied on both sides of the solar cells using screen printing or jet dispensing, the wires on both sides are individually connected to two thin metal ribbons at either end of the solar cell. The final stringing can be afterwards simply achieved by overlapping and connecting these ribbons in series. This Direct Wire Bonding approach presents a promising pathway for cost reduction and performance enhancement in next-generation solar cell modules.

CRediT authorship contribution statement

Yanxin Liu: Writing – review & editing, Writing – original draft, Methodology, Investigation, Data curation, Conceptualization. **Ian Marius Peters:** Supervision. **Kaining Ding:** Supervision. **Bart Pieters:** Supervision. **Karsten Bittkau:** Supervision. **Uwe Rau:** Supervision. **Mohamed Issifi Yacouba:** Data curation. **Henrike Gattermann:** Writing – review & editing. **Volker Lauterbach:** Investigation. **Andreas Lambertz:** Writing – review & editing, Supervision.

Declaration of generative AI and AI-assisted technologies in the writing process

During the preparation of this work the author(s) used DeepL in order to improve the language and readability. After using this tool/service, the author(s) reviewed and edited the content as needed and take(s) full responsibility for the content of the publication.

Declaration of competing interest

The authors declare that they have no known competing financial interests or personal relationships that could have appeared to influence the work reported in this paper.

Acknowledgement

We appreciate the financial support of Bundesministerium für Wirtschaft und Klimaschutz through the TOP Project [03EE1080B].

Data availability

Data will be made available on request.

References

[1] THE PARIS AGREEMENT. https://treaties.un.org/Pages/ViewDetails.aspx?src=TREATY&mtdsg_no=XXVII-7, 2016.
[2] ITRPV 15th Edition Presentation, n.d. https://www.vdma.org/international-technology-roadmap-photovoltaic (accessed July 12, 2024).
[3] Y. Zhang, M. Kim, L. Wang, P. Verlinden, B. Hallam, Design considerations for multi-terawatt scale manufacturing of existing and future photovoltaic technologies: challenges and opportunities related to silver, indium and bismuth consumption, Energy Environ. Sci. 14 (2021) 5587–5610, https://doi.org/10.1039/d1ee01814k.
[4] U. National Minerals Information Center, Bismuth Data Sheet - Mineral Commodity Summaries 2020, n.d.
[5] Y.C. Chang, Y. Zhang, L. Wang, S. Wang, H. Wang, C.Y. Huang, R. Chen, C. Chan, B. Hallam, Silver-lean metallization and hybrid contacts via plating on screen-printed metal for silicon solar cells manufacturing, in: Progress in Photovoltaics: Research and Applications, John Wiley and Sons Ltd, 2024, https://doi.org/10.1002/pip.3799.
[6] B.E. Pieters, A free and open source finite-difference simulation tool for solar modules, in: 2014 IEEE 40th Photovoltaic Specialist Conference, 2014, https://doi.org/10.1109/PVSC.2014.6925173. PVSC 2014.
[7] W.M. Loh, S.E. Swirhun, T.A. Schreyer, K.C. Saraswat, R.M. Swanson, Modeling and measurement of contact resistances, IEEE Trans Electron Devices 34 (1987), https://doi.org/10.1109/T-ED.1987.22957.
[8] J.E. Park, W.S. Choi, D. Lim, Cell/module integration technology withwire-embedded EVA sheet, Appl. Sci. 11 (2021), https://doi.org/10.3390/app11094170.
[9] A. Lachowicz, A. Descoeudres, J. Champliaud, A. Faes, J. Geissbühler, M. Despeisse, S. Nicolay, C. Ballif, COPPER PLATING PROCESSES FOR SILICON HETEROJUNCTION SOLAR CELLS: AN OVERVIEW, n.d.